The International Journal of Advanced Manufacturing Technology (2019) 100:3197–3206
https://doi.org/10.1007/s00170-018-2926-5

ORIGINAL ARTICLE

Feature selection and a method to improve the performance of tool condition monitoring

Zhengyou Xie[1] · Jianguang Li[1] · Yong Lu[1]

Received: 4 May 2018 / Accepted: 23 October 2018 / Published online: 29 October 2018

Abstract
Tool condition monitoring (TCM) is especially important in the modern machining process. In order to distinguish different tool wear states accurately and reduce the computation cost, it is of great significance to extract and select appropriate features that can reflect changes in tool wear states but are insensitive to cutting parameters. In this work, Fisher's discriminant ratio (FDR) is adopted as the criterion for feature selection by evaluates every feature's classification ability. However, it is found that the continuous hidden Markov models (CHMM) trained based on the features selected by the conventional method could recognize some tool state well, but have poor ability to classify other wear states. The reasons for this phenomenon have been analyzed, then a simple and effective method that used two feature sets for TCM has been proposed to improve the recognition performance. Four tests with different cutting parameters are carried out, and the new method has been implemented and verified its usefulness and validity.

Keywords Feature selection · Fisher's discriminant ratio · Hidden Markov model · Tool condition monitoring · Cutting force · Tool wear

1 Introduction

Cutting tool wear can undermine machining efficiency, processing accuracy, and surface quality of workpieces to a certain extent, thus tool condition monitoring (TCM) is of great significance during cutting process and has attracted much attention from researchers for decades [1].

A complete TCM process mainly consists of signal acquisition, feature extraction, and system identification [2]. The signals commonly used for TCM include cutting force [3], cutting vibration [4], acoustic emission [5], and motor current or power [6], which have all been proved feasible to some extent, and among which cutting force is the most widely applied signal. As for system identification, artificial neural networks (ANN) and support vector machines (SVM) have been used widely [2]. Besides, hidden Markov model (HMM) with strict data structures and reliable computing performance has also attracted lots of attentions. In recent years, many researchers have applied HMM in TCM and achieved good results [3, 7].

The raw signal during cutting process has a lot of useless information including noise. For reliably and effectively monitoring tool condition, a variety of features in time, frequency, and time-frequency domains have been extracted and researched. In order to reduce the computation cost and improve TCM model robustness, it is necessary to select feature subset from numerous features that can reflect changes in tool wear states but are insensitive to cutting parameters. As a result, various feature selection algorithms have been proposed.

Some researchers applied the Pearson correlation coefficient to find the features that can best characterize tool wear conditions [8, 9]. However, this method was based on uncertain assumption that the correlation between features and tool wears was linear [1]. Zhu et al. [10] modified the Fisher's linear discriminant analysis for feature selection. They used the Fisher's discriminant ratio (FDR) to evaluate each feature's class-discriminant ability. For calculating FDR, no

✉ Yong Lu
luyhit@163.com

Zhengyou Xie
xiezhengyou@126.com

Jianguang Li
mejgli@hit.edu.cn

[1] School of Mechatronics Engineering, Harbin Institute of Technology, Harbin, China

specific tool wear values are required, just need to determine the tool wear states. The approach was also compared with principal component analysis (PCA) and automatic relevance determination (ARD) and showed superiority in HMM modeling. Geramifardet al. [11] have also conducted a comparative study about FDR with other three feature selection methods for TCM, which are ridge regression (RR), principal component regression (PCR), and least absolute shrinkage and selection operator (LASSO).Applicability of these methods are compared based on their diagnostic results in two cases using a single hidden Markov model (HMM) approach, and the FDR has a good performance. Due to the effectiveness of the FDR-based feature selection method, it has gained many applications in TCM [12–14].

However, the selected feature may not be the optimal set to classify all states in practical applications, if calculating the FDR of each feature directly using the data from all classes just like in [10–14]. In this paper, FDR is also adopted as the criterion to select the appropriate features to recognize different tool states. It is found that the features selected by the conventional method could distinguish some tool state well, but have poor ability to classify other wear states. The reasons for this phenomenon have been analyzed, and a simple and effective method to improve the performance of tool condition monitoring has been proposed.

The paper is organized as follows: in Section 2, the experimental work is done, and cutting force and tool wear data in different cutting parameters under the tool full life cycle are acquired for subsequent analysis. Then the features are extracted and selected according to their FDR values. Section 3 shows the construction work of tool wear states monitoring based on CHMM. The results are analyzed and the discussion about the poor recognition ability on some states is provided in Section 4. In Section 5, a method to improve the TCM performance is proposed, and its performance is verified. Finally, the conclusions are given in Section 6.

2 Experimental work and feature selection

2.1 Experimental work and data acquisition

In order to obtain enough cutting force data in different tool wear condition to research TCM, experiments have to be carried out. In this paper, the work was performed on a vertical machining center (VMC1600B) by end milling 45 steel under dry cutting condition. Experiment setup is illustrated in Fig. 1. The cutting force was measured by the smart tool holder system developed by the authors in the previous study [15], which is capable of measuring triaxial cutting force and a torque simultaneously in a wireless environment system with a sampling rate of 5000 Hz. In this study, the cutting forces in three directions were chosen and collected as the raw signal for further analysis. The smart tool holder was equipped with a 32-mm diameter cutter arbor (BAP400R-35-160-C32) and a PVD coated carbide insert (Mitsubishi APMT1604PDER). The tool insert wear was measured using a microscope. After getting the force and tool wear data, the features were extracted and selected, and then models were constructed for TCM.

The experiments were conducted in different machining conditions as listed in Table 1 with different spindle speed and feed per tooth. There are four tests and each one for a new tool insert. The cutting tool inserts are usually replaced when the width of the flank wear area (VB) reaches some predefined limit. According to ISO 8688, the threshold for determining the tool life is maximum flank wear of 0.3 mm in conventional machining [16]. During the cutting process, the VB value was measured once finished a sample length of cutting until the tool wear reached 0.3 mm. As a result, the force and wear data of four inserts in total in different cutting parameters under the full life cycle can be acquired in this study. Moreover, the tool wear was divided into three states, named initial worn (0–0.11 mm), medium worn (0.11–0.23 mm), and severe worn (0.23–0.30 mm) based on the experiment data by using tool wear rate as the criterion. In initial worn state and severe worn state, the tool has a faster wear rate than that in medium worn state. Cutting tool inserts in different wear conditions were shown in Fig. 2.

2.2 Feature extraction and selection

Due to the intermittent cutting process of milling, the cutting forces are typically time varying and nonstationary. The raw signal collected by the smart tool holder included not only the useful tool wear–related information but also the noise and the information caused by the changes of the cutting parameters, thus it cannot be directly used for TCM. Features have to be extracted from the force data for robust and effective representation.

Time-domain features are firstly extracted to show the force statistics, like mean, root mean square, variance, skewness, kurtosis, crest factor, and dynamic component. These features have been adopted by many researchers to monitor tool condition and achieved some results. In addition, wavelet analysis, especially wavelet packet decomposition (WPD), has been proved effective in processing the nonstationary signal. It was found that WPD coefficients include large valuable information which is sensitive to tool wear and little influenced by the variation of working conditions [17]. Features extracted from the wavelet coefficients are widely used for TCM. Among them, the energy of each frequency band after WPD has attracted a lot of attention [18]. Besides, other statistics of WPD coefficients, like root mean square, variance, kurtosis, and crest factor have also been researched. In this

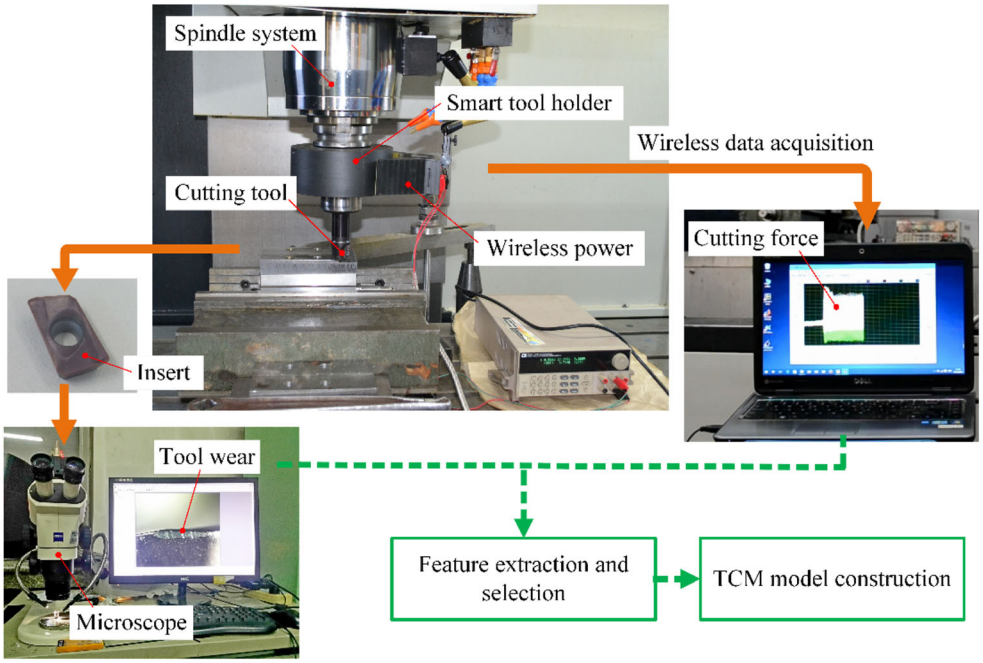

Fig. 1 Experiment setup

study, all these features in time domain and wavelet domain are extracted from the origin cutting force signal. Due to the Daubechies wavelet's advantages of orthogonality, compact support in the time domain, and computational simplicity, the signal was decomposed using db4 wavelet packet into three levels. The coefficients in the third level, $2^3 = 8$ scales in total, were selected. Forty-seven features have been calculated in each direction's force as list in Table 2. As a result, a total of 141 features were extracted from F_x, F_y, and F_z.

Where $\{x_i\}$, $i = 1, \cdots, N$ is feature sample set, N is the number of the samples, and σ is the set's standard deviation. x_{amp} is amplitude of raw force; x_{med} is mean force of the segment [19]. $\left\{d_{j,k}^n\right\}, n = 1, \cdots, N_j$ is the set of the wavelet coefficients in the jth level and kth scale, N_j is the number of coefficients at jth level, and $j = 3$ in this work.

The purpose of feature selection is to find an appropriate subset of features that can explicitly discriminate different tool wear conditions. Therefore, the selected features should have great differences between different categories and similarities in the same category. Since the Fisher discriminant ratio (FDR) can be used to rank the class-discriminant ability of the features as mentioned before, it was adopted for feature selection in this paper. A modified computational formula of FDR introduced [10] is shown as follows:

$$\mathrm{FDR}(m) = \frac{\mathrm{SB}^m}{\mathrm{SW}^m} = \frac{\sum_{i=1}^{K}\sum_{j=1}^{K}\left(\mu_i{}^m - \mu_j{}^m\right)^2}{\sum_{i=1}^{K} s_i{}^m} \tag{1}$$

where m is the serial number of the features, and K is the number of classes. SB^m and SW^m are the scatter between and scatter with of the mth feature. $\mu_i{}^m$ is the mean value of the mth feature in the ith class C_i, which and s_i can be calculated with

$$\mu_i{}^m = \frac{1}{n_i}\sum_{x \in C_i} x \tag{2}$$

$$s_i = \sum_{x \in C_i}\left(x - \mu_i{}^m\right)\left(x - \mu_i{}^m\right)^T \tag{3}$$

where x is the feature samples which belongs to the class C_i, and n_i is the feature numbers in this class.

To compute the features' FDR values, 10 s force data from each tool wear state in *Test 1* were taken and

Table 1 Experiment cutting parameters

Test number	Spindle speed (r/min)	Feed per tooth (mm/Z)	Axial depth of cut (mm)	Radial depth of cut (mm)
1	1600	0.10	0.5	16
2	1600	0.15		
3	1900	0.10		
4	2200	0.10		

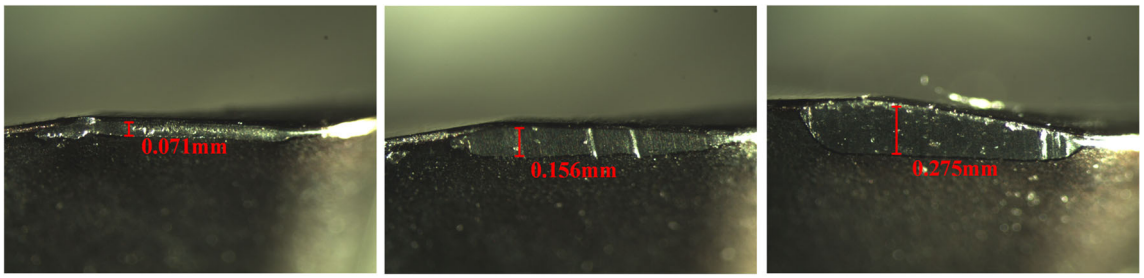

Fig. 2 Cutting tools in different wear states: **a** initial worn, **b** medium worn, and **c** severe worn

processed. It should be noted that there are large differences in values between different features due to their different dimensions and sources. Thus, all 141 features need to be normalized into the [0, 1] interval firstly. After calculating all the FDR values, the features are ranked in descending order as demonstrated in Fig. 3.

There are two knee points at 5 and 10, as a rule of thumb, these two may be the appropriate choice as the number of features to be adopted from 141 features. Features with top 14 FDR values, nearly top 10%, were achieved as listed in Table 3, where the Decrease column represents the percentage reduction of the current feature's FDR value compared to the previous one. Considering that the 11th feature's FDR has dropped to a particularly small value, top 10 features were selected for TCM in this paper.

Moreover, as can be seen from Table 3, the axial force F_z is more sensitive to tool wear conditions, as the first six features are all from F_z, and the next four are from radial force F_x. This was in agreement with Zhu [14], in whose work TCM was studied based on the analysis of singularity of cutting force waveforms, and the F_z component of the cutting force was proved more effective and stable than F_x and F_y.

Table 2 Features extracted from cutting force

Domain	Number	Feature	Formula
Time domain	1	Mean (μ)	$\mu = \frac{1}{N}\sum_{i=1}^{N} x_i$
	2	Root mean square (Rms)	$\mathrm{Rms} = \sqrt{\frac{1}{N}\sum_{i=1}^{N} x_i^2}$
	3	Variance (Var)	$\mathrm{Var} = \frac{1}{N}\sum_{i=1}^{N} (x_i - \mu)^2$
	4	Skewness (Ske)	$\mathrm{Ske} = \frac{1}{N}\sum_{i=1}^{N} (x_i - \mu)^3 / \sigma^3$
	5	Kurtosis (Kur)	$\mathrm{Kur} = \frac{1}{N}\sum_{i=1}^{N} (x_i - \mu)^4 / \sigma^4$
	6	Crest factor (Cf)	$\mathrm{Cf} = \frac{\max\lvert x_i\rvert}{\mathrm{Rms}}$
	7	Dynamic component (Dc)	$\mathrm{Dc} = \lvert x_{\mathrm{amp}} - x_{\mathrm{med}}\rvert$
Wavelet domain	8–15	WPD energy ($\mathrm{wE_k}$)	$\mathrm{wE_k} = \frac{1}{N_j}\sum_{n=1}^{N_j}\left[d_{j,k}^n\right]^2, k = 1, \cdots, 8$
	16–23	WPD coefficient Rms (wcRms)	$\mathrm{wcRms_k} = \sqrt{\frac{1}{N_j}\sum_{n=1}^{N_j}\left[d_{j,k}^n\right]^2}$
	24–31	WPD coefficient Var (wcVar)	$wcVar_k = \frac{1}{N_j}\sum_{n=1}^{N_j}\left[d_{j,k}^n - \overline{d_{j,k}}\right]^2$
	32–39	WPD coefficient Kur (wcKur)	$\mathrm{wcKur_k} = \frac{1}{N_j}\sum_{n=1}^{N_j}\left[d_{j,k}^n - \overline{d_{j,k}}\right]^4 / {\sigma_{j,k}}^4$
	40–47	WPD coefficient Cf (wcCf)	$\mathrm{wcCf}_k = \frac{\max\lvert d_{j,k}\rvert}{\mathrm{wcRms}_k}$

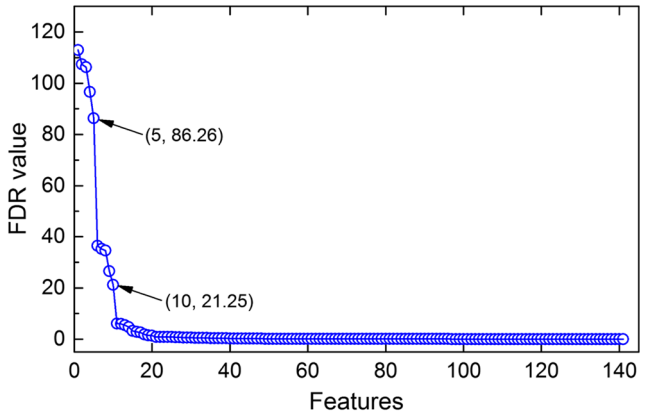

Fig. 3 FDR values of all the features in descending order

3 CHMM for tool wear condition monitoring

HMM describes a double stochastic process that includes an underlying finite-state hidden Markov process and an observable process associated with the hidden states. In the tool state monitoring, the tool wears are regarded as hidden states for cannot be directly observed, while observations are the features extracted from cutting force. HMM is mature and has been used by many researchers for TCM as mentioned earlier. The author has also applied HMM to diagnose tool wear conditions based on cutting vibration signal and achieved good results in the previous work [20].

The framework of HMM was demonstrated in Fig. 4, where there are two processes: training process and recognition process. In the first process, the features that are strongly correlated with tool wear state are extracted and used to train HMM based on the expectation-maximization (EM) algorithm [21], and three HMMs would be established for three different wear states of the tool, denoted as HMM1, HMM2, and HMM3. Then in the recognition process, when an unknown tool wear state needs to be identified, the same features used in training process were extracted and then sent to each model to calculate the likelihoods using Viterbi algorithm. The model in three with the largest likelihood value can be considered that the current tool belongs to this wear state.

Table 3 Features with top 10 FDR values

Order	Feature	FDR	Decrease (%)
1	Z-wE$_1$	112.84	–
2	Z-Rms	107.39	4.83
3	Z-wcRms$_1$	106.31	1.01
4	Z-wcVar$_1$	96.55	9.18
5	Z-Var	86.26	10.65
6	Z-μ	36.32	57.90
7	X-wcRms$_1$	35.11	3.33
8	X-wE$_1$	34.52	1.68
9	X-wcVar$_1$	26.60	22.94
10	X-μ	21.25	20.12
11	Y-wpe1	6.09	71.32
12	Y-wcRms$_1$	5.90	3.10
13	Y-wcVar$_1$	5.40	8.58
14	X-rms	4.68	13.33

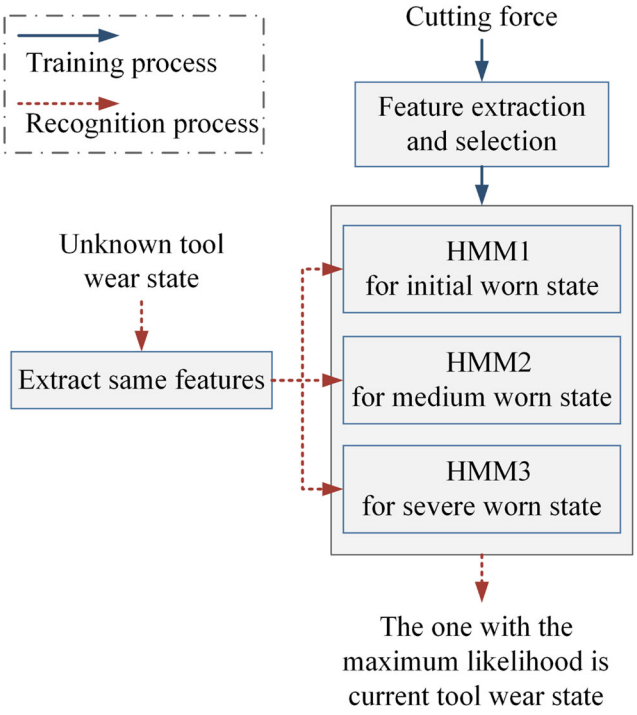

Fig. 4 Framework of HMM for TCM

Due to the statistical characteristics of the observations and always increasing tool wear, the left-right continuous HMM was chosen in this paper. A CHMM can be represented as $\lambda = \{\pi, A, \mu_{jm}, U_{jm}, c_{jm}\}$, where π is the initial state probability distribution vector, in this paper $\pi = [1\ 0\ 0\ 0\ 0]$ for the state number was preliminary set to 5. A is the hidden state transition probability matrix, and for next step iterative training, it is initialized as follows:

$$A_0 = \{a_{ij}\}_{5\times5} = \begin{cases} 0.5 & j = i \text{ or } j = i+1, \quad 1 \le i \le 4 \\ 1 & i = j = 5 \\ 0 & \text{others} \end{cases}$$

For CHMM, the probability distribution of observation sequence can be represented by a Gaussian mixture model (GMM). Theoretically, a GMM can approximate any signal to a certain precision when provided with enough mixture components. M is the number of Gaussian components, which was set $M = 3$; here, c_{jm} is the mixture coefficient, μ_{jm} is the mean matrix, and U_{jm} is the covariance matrix.

To gain features, the force signal needs to be segmented into a sequence of observations. Too large segment window may cause more time to compute, which would affect the real-time ability of TCM system. However, if the window is too

Table 4 Recognition results

Recognition accuracy rate in different test (%)					
	Test 1	Test 2	Test 3	Test 4	Average rate
Initial worn	90.0	82.0	92.9	90.8	88.3
Medium worn	78.3	88.2	81.4	83.3	82.6
Severe worn	97.3	92.0	91.4	91.4	93.6

small, the signal is not stable and cannot be extracted effective information. In this study, the sampled cutting force signals were processed with a window segment of 500 points, which is equivalent as about three revolutions of the cutter and corresponding period of 0.1 s.

4 Results analysis and discussion

Some force data were taken from *Test 1*, and 10 features listed in Table 3 were extracted and used to train the three HMMs. In recognition process, samples random selected from all four tests were extracted the same features and then put into three models to calculate the likelihoods and recognize the tool wear states. Notice that the data for recognition in *Test 1* were randomly selected from what were not used for model training. The recognition results were shown in Table 4.

The recognition accuracy rate of the tool in severe worn state was the best with a maximum value of 97.3% in *Test 1* and an average value of over 93%, while initial worn tool and medium worn tool were classified a trifle worse. To further analyze this phenomenon, 60 samples from the identification data of *Test 3* (20 samples for each tool state) were selected and plotted as exhibited in Fig. 5.Different colors and symbols represent different models. The unknown tool worn was considered as the wear state of which the model had the maximum likelihood. For instance, in Fig. 5a, when sample number = 1, the likelihood value under HMM1, the circle symbol in blue is the largest, which means the sample is identified as the state corresponding to HMM1, that is, the initial worn state. All samples in Fig 5a are from the initial worn data, thus the identification result of the first sample is correct.

In Fig. 5a, three samples are wrong classified and recognized as the medium worn state, and five samples in Fig. 5b are recognized as the initial worn state incorrectly. Moreover, the likelihood values of those samples under HMM1 and HMM2 in Fig. 5a, b are very similar. This is probably due to that the features selected in Section 2.2 have poor performance to classify the first two wear states. To verify this hypothesis, more analysis is necessary.

In Section 2.2, the FDR values, recorded as $FDR_{I\text{-}M\text{-}S}$ here, were calculated using the force data from all three-tool wear states, reflecting the features' average classification

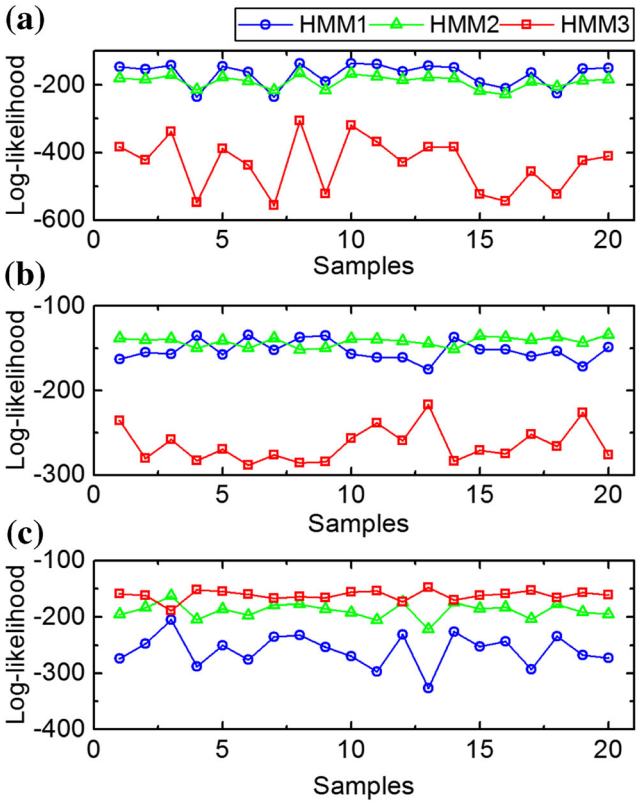

Fig.5 **a** Initial worn, **b** medium worn, and **c** severe worn tool wear states recognition results

performance of these three categories. To find the feature subset that can better classify initial worn and medium worn states, only take force data from these two states and compute each feature's FDR, denoted as $FDR_{I\text{-}M}$ here. Meanwhile, $FDR_{M\text{-}S}$ is also calculated by the data only from medium worn and severe worn for comparison analysis. Respective 10 features with top values are achieved as listed in Table 5. The corresponding FDR values are shown in the Fig. 6. The solid

Table 5 Top 10 features in descending order of respective FDR values

Ordered by $FDR_{I\text{-}M\text{-}S}$		Ordered by $FDR_{I\text{-}M}$		Ordered by $FDR_{M\text{-}S}$	
Number	Feature	Number	Feature	Number	Feature
1	Z-wE_1	4	Z-$wcVar_1$	2	Z-Rms
2	Z-Rms	5	Z-Var	1	Z-wE_1
3	Z-$wcRms_1$	11	Y-μ	3	Z-$wcRms_1$
4	Z-$wcVar_1$	3	Z-$wcRms_1$	4	Z-$wcVar_1$
5	Z-Var	1	Z-wE_1	5	Z-Var
6	Z-μ	2	Z-Rms	6	Z-μ
7	X-$wcRms_1$	12	Y-Rms	7	X-$wcRms_1$
8	X-wE_1	13	Y-wE_1	9	X-$wcVar_1$
9	X-$wcVar_1$	14	Y-$wcRms_1$	8	X-wE_1
10	X-μ	15	Y-Var	10	X-μ

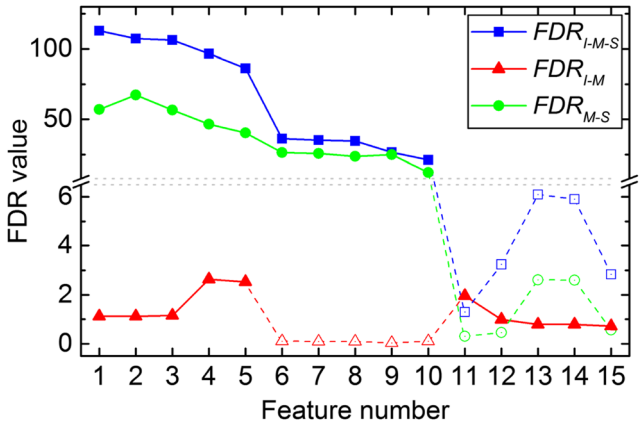

Fig. 6 FDR values of features calculated by three different methods

symbols on solid lines represent the selected features, and the hollow ones on dash lines are not selected.

The top 10 features ordered by $FDR_{I\text{-}M\text{-}S}$ values and the ones by $FDR_{M\text{-}S}$ are the same, except slight difference in the values and sorting, see Table 5 and Fig. 6. Moreover, these two group FDR values are much larger than $FDR_{I\text{-}M}$. It shows that compared to the difference between severe worn and the other two wear states, the features between initial worn and medium worn have less differences. This leads to the fact that in the selection of features which can classify the three states, the actual selected features can mainly recognize severe worn state, and some features that can better identify initial worn and medium worn are not selected. This situation exists that different features have different ability to recognize different tool states. Liao et al. [22] has observed that the kurtosis of wavelet coefficients can easily distinguish severe worn condition while it has no distinct difference between initial worn and medium worn.

As can be seen from Table 5, there are five new features, marked in italics, in top 10 ordered by $FDR_{I\text{-}M}$ values, which are all from Y-direction cutting force. In order to visually observe the difference of the two sets of features, $\{Features\}_{I\text{-}M\text{-}S}$ and $\{Features\}_{I\text{-}M}$, between the three categories, 150 samples of features, 50 for each tool wear state, were extracted from force data in *Test 1* and analyzed. The two feature sets were both ten-dimensional, so they were reduced to two dimensions based on PCA to plot and display. The $\{Features\}_{I\text{-}M\text{-}S}$ and $\{Features\}_{I\text{-}M}$ sets in two-dimensional space were shown in Fig. 7. It should be noted that a little bit of information would be lost after dimension reduction, but it still can basically reflect the distribution of original multi-dimensional features in different categories.

In Fig. 7a, features from three-tool wear states show different distribution, especially that from severe worn tool, which is far away from other two states. Moreover, the features from initial worn tool and that from medium worn are very close in distribution. It undoubtedly means $\{Features\}_{I\text{-}M\text{-}S}$ could distinguish out severe worn tool well, but classify between initial worn and medium worn tools worse, which is consistent with the previous recognition results in Table 4. While in Fig. 7b, the distance between first two categories is expanded, but shortened between medium worn and severe worn tools. To assess the classification effect of the new feature set $\{Features\}_{I\text{-}M}$, they were also taken to conduct model training, and the new model set $\{HMM_1, HMM_2, HMM_3\}_{I\text{-}M}$ was obtained and used for TCM.

For comparison, the data used in this training is the same as the previous one, and the identification data were the 60 samples in Fig. 6. The test results are shown in Fig. 8. The samples in the rectangle were the ones whose recognition results were changed. The tests show that the identification results of the first two wear states have improved, while the recognition accuracy of the third state has decreased, which means that the newly selected features are indeed better able to identify initial worn and medium worn states. This can be used to improve the accuracy of TCM. The specific method is described in the following section.

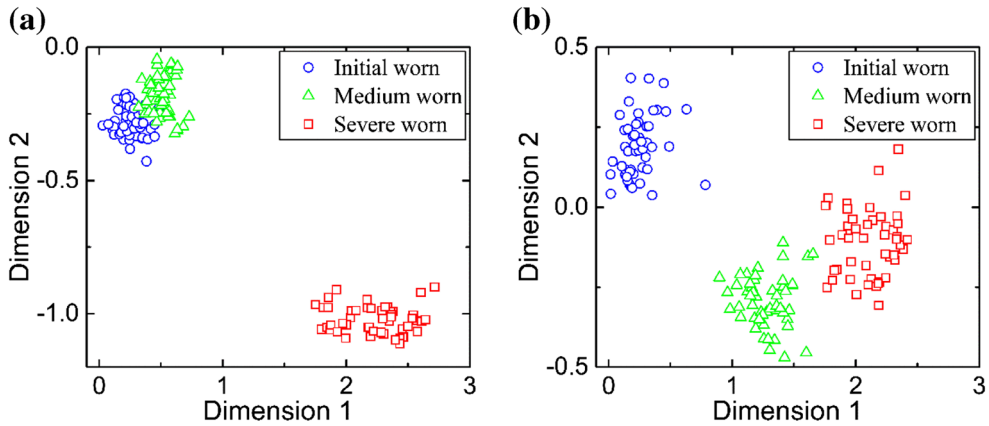

Fig. 7 **a** $\{Features\}_{I\text{-}M\text{-}S}$ and **b** $\{Features\}_{I\text{-}M}$ sets in two-dimensional space

5 Method for TCM performance promotion

5.1 Method introduction and implement

Since some features can identify the severe worn condition well and some others has good ability to discriminate between initial worn and medium worn states, it probably be a good choice to use two sets of features to monitor tool wear states. The flowchart of the new method, re-recognize based on different features, rR-DF for short here, is illustrated in Fig. 9. The key point of the method rR-DF is to select two appropriate sets of features to train two model sets. When an unknown tool wear state needs to be identified, use one model set to determine whether the state belongs to severe worn. If not, use another model set to re-recognize if the tool wear is initial worn or medium worn.

5.2 Performance verification

In order to verify the reliability of the rR-DF method for improving the performance of tool wear condition monitoring, the data from all four cutting tests listed in Table 1 were taken for identification. The results are summarized in the Table 6. The data in *Comparison* rows refers to the improvements of recognition accuracy rate based on the new method compared to the results in Table 4.

As the rR-DF method only re-recognizes initial worn and medium worn tool states, the recognition rate of severe worn remains unchanged, marked as "→" in the table. However, it shows obvious improvements on discrimination of the first-two wear states, marked as "↑." Compare to recognizing initial worn tool, the proposed method can better improve the medium worn recognition accuracy, and the maximum value of increment was 13.4% occurred in *Test 1*. Overall, the recognition rates of the initial worn and medium worn states in four cutting

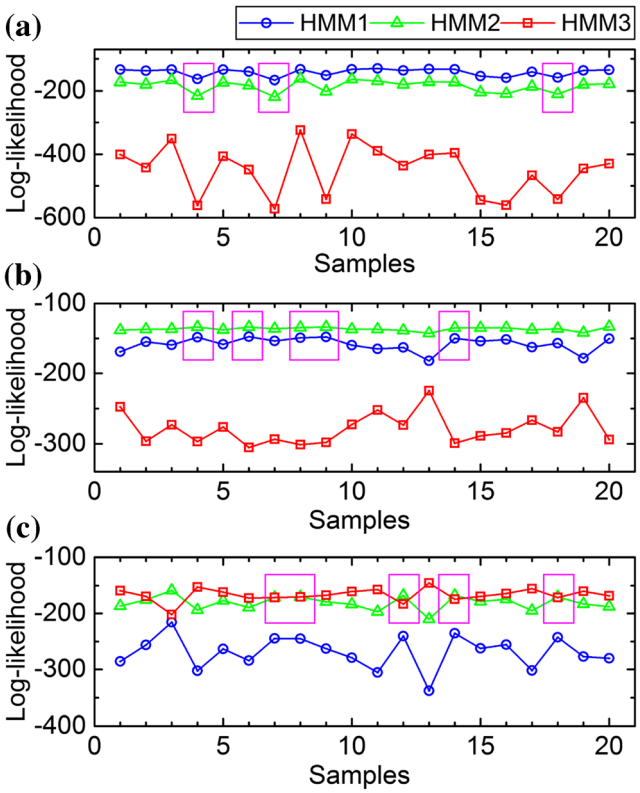

Fig. 8 **a** Initial worn, **b** medium worn, and **c** severe worn tool wear states recognition results based on $\{Features\}_{I\text{-}M}$

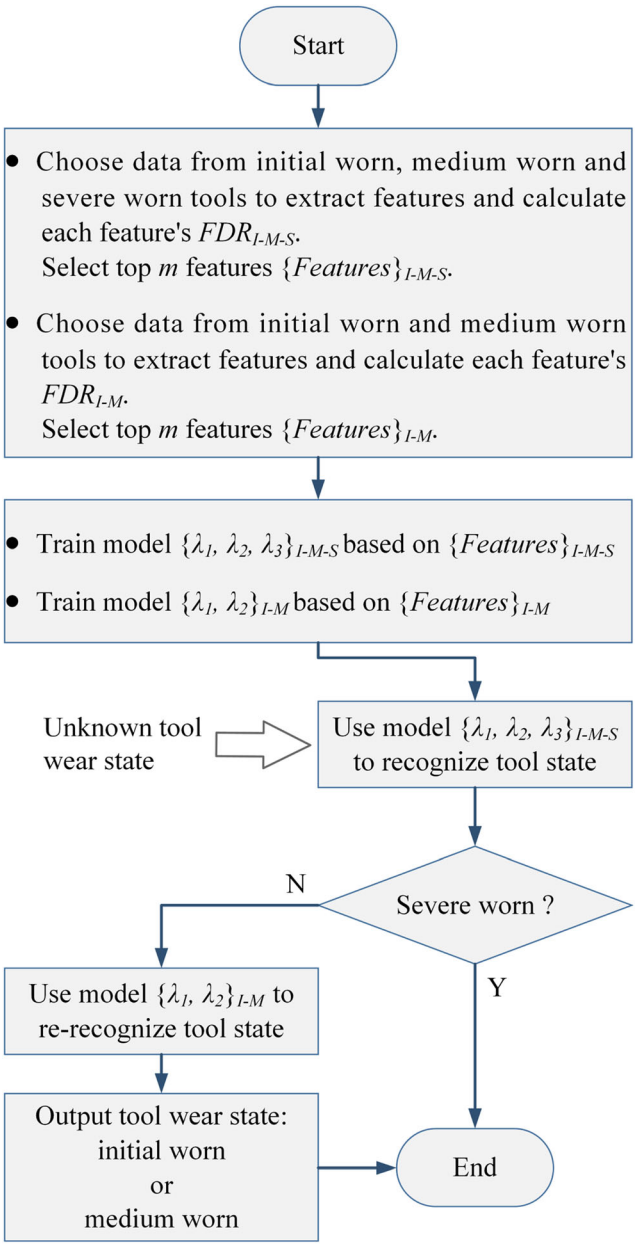

Fig. 9 Flowchart of the new method rR-DF

Table 6 Recognition results based on rR-DF

		Test 1	Test 2	Test 3	Test 4	Average rate
Initial worn	Recognition rate (%)	90.0	91.0	97.1	92.3	92.6
	Comparison (%)	→	↑ 9.0	↑ 4.2	↑ 1.5	↑ 3.7
Medium worn	Recognition rate (%)	91.7	91.8	91.4	90.0	91.2
	Comparison (%)	↑ 13.4	↑ 3.6	↑ 10	↑ 6.7	↑ 8.4
Severe worn	Recognition rate (%)	97.3	92.0	91.4	91.4	93.0
	Comparison (%)	→	→	→	→	→

tests have increased by an average of 3.7% and 8.4%, respectively. Also, the new method has reduced the influence of cutting parameters on the monitoring model to some extent, and improved the robustness of the system, resulting in that the recognition accuracy rates of all the tool wear states in all the tests are above 90%.

6 Conclusions and future work

In this paper, multiple sets of cutting experiments have been conducted in order to obtain cutting force and wear data to facilitate tool wear monitoring research in the next step. Numerous time domain and wavelet domain features were extracted, and their FDR values were calculated to assess their classification ability. The 10 features with top values were selected and used to establish the CHMMs to recognize the tool wear conditions. The results show the selected features could distinguish severe worn tool state well, but have poor ability to classify other states. This is mainly due to that the FDR calculated using the force data from all three-tool wear states reflects the average classification performance of these three categories, and some features which can better classify initial worn and medium worn states were not selected. Thus, a simple and effective method to improve the recognition performance has been proposed. The new idea of this method is using two different feature sets to monitor different tool wear conditions. The specific implementation step was introduced, and it was verified by four cutting tests with different cutting parameters. The recognition results show that the proposed new method does effectively improve the TCM performance. The recognition accuracy rate of the initial worn and medium worn states increased by an average of 3.7% and 8.4%, respectively.

Nevertheless, there are still some improvements that can be made in future work. The authors intend to analyze more kinds of signals during cutting process, like cutting vibration and acoustic emission, etc., to extract more features for TCM, and more features will be evaluated their classification ability based on FDR. Besides, the proposed method avoids the need to find or construct new features to classify all categories, and obtain good identification results only using common features by two-step classifying. Whether this method can be applied to other areas of pattern recognition is worth studying.

Funding information This work was supported by the National High Technology Research and Development Program of China (863 Program) under Grant No. 2013AA041107.

References

1. Teti R, Jemielniak K, O'Donnell G, Dornfeld D (2010) Advanced monitoring of machining operations. CIRP Ann Manuf Technol 59(2):717–739
2. Kong D, Chen Y, Li N (2018) Gaussian process regression for tool wear prediction. Mech Syst Signal Process 104:556–574
3. Liao Z, Gao D, Lu Y, Lv Z (2016) Multi-scale hybrid HMM for tool wear condition monitoring. Int J Adv Manuf Technol 84(9–12): 2437–2448
4. Sevilla-Camacho PY, Robles-Ocampo JB, Muñiz-Soria J, Lee-Orantes F (2015) Tool failure detection method for high-speed milling using vibration signal and reconfigurable bandpass digital filtering. Int J Adv Manuf Technol 81(5–8):1187–1194
5. Wu H, Yu Z, Wang Y (2016) Real-time FDM machine condition monitoring and diagnosis based on acoustic emission and hidden semi-Markov model. Int J Adv Manuf Technol 1–10
6. Sevilla-Camacho PY, Herrera-Ruiz G, Robles-Ocampo JB, Jáuregui-Correa JC (2011) Tool breakage detection in CNC high-speed milling based in feed-motor current signals. Int J Adv Manuf Technol 53(9–12):1141–1148
7. Yu J, Liang S, Tang D, Liu H (2016) A weighted hidden Markov model approach for continuous-state tool wear monitoring and tool life prediction. Int J Adv Manuf Technol 91(1–4):1–11
8. Zhang C, Yao X, Zhang J, Jin H (2016) Tool condition monitoring and remaining useful life prognostic based on a wireless sensor in dry milling operations. Sensors 16(6):795
9. Scheffer C, Heyns PS (2004) An industrial tool wear monitoring system for interrupted turning. Mech Syst Signal Process 18(5): 1219–1242
10. Zhu KP, Hong GS, Wong YS (2008) A comparative study of feature selection for hidden Markov model-based micro-milling tool wear monitoring. Mach Sci Technol 12(3):348–369
11. Geramifard O, Xu JX, Zhou JH, Li X (2012) Feature selection for tool wear monitoring: a comparative study. In: Industrial electronics and applications. p 1230–1235

12. Bhat NN, Dutta S, Pal SK, Pal S (2016) Tool condition classification in turning process using hidden Markov model based on texture analysis of machined surface images. Measurement 90:500–509
13. Geramifard O, Xu JX, Zhou JH, Li X (2012) A physically segmented hidden Markov model approach for continuous tool condition monitoring: diagnostics and prognostics. IEEE Trans Ind Inf 8(4):964–973
14. Zhu K, Hong GS, San WY (2011) Multiscale singularity analysis of cutting forces for micromilling tool-wear monitoring. IEEE Trans Ind Electron 58(6):2512–2521
15. Xie Z, Lu Y, Li J (2017) Development and testing of an integrated smart tool holder for four-component cutting force measurement. Mech Syst Signal Process 93:225–240
16. Organization IS (1989) Tool life testing in milling—Part 2: End milling. ISO 8688-2: 1989
17. Zhu K, Wong YS, Hong GS (2009) Wavelet analysis of sensor signals for tool condition monitoring: a review and some new results. Int J Mach Tool Manu 49(7):537–553
18. Wang M, Wang J (2012) CHMM for tool condition monitoring and remaining useful life prediction. Int J Adv Manuf Technol 59(5–8):463–471
19. Zhu K, Wong YS, Hong GS (2009) Multi-category micro-milling tool wear monitoring with continuous hidden Markov models. Mech Syst Signal Process 23(2):547–560
20. Xie Z, Li J, Lu Y (2018) An integrated wireless vibration sensing tool holder for milling tool condition monitoring. Int J Adv Manuf Technol 95(5–8):2885–2896
21. Rabiner LR (1990) A tutorial on hidden Markov models and selected applications in speech recognition, readings in speech recognition. Morgan Kaufmann, San Francisco, pp 267–296
22. Gao D, Liao Z, Lv Z, Lu Y (2015) Multi-scale statistical signal processing of cutting force in cutting tool condition monitoring. Int J Adv Manuf Technol 80(9–12):1843–1853